

Inclusive cross-sections for jet production in nucleus-nucleus collisions in perturbative QCD

M.A.Braun

Dep. of High Energy physics, University of S.Petersburg,
198504 S.Petersburg, Russia

July 14, 2018

Abstract. Inclusive cross-sections for gluon jet production are studied numerically in the perturbative QCD pomeron model for central collisions of identical nuclei at high energies. Two forms for the inclusive cross-sections, with and without emission from the triple pomeron vertex, are compared. The difference was found to reduce to a numerical factor $0.8 \div 0.9$ for momenta below the saturation momentum Q_s . Above Q_s no difference was found at all. The gluon spectrum was found to be $\sim A$ at momenta k below Q_s and $\sim A^{1.1}$ above it. At large k the spectrum goes like $1/k^{2.7 \div 3.3}$ flattening with energy. The multiplicities turned out to be proportional to A with a good precision. Their absolute values are high and grow rapidly with energy in accordance with the high value of the BFKL intercept.

1 Introduction

In view of the new experimental data on heavy-ion collisions at RHIC and future such data to be obtained at LHC one would like to have predictions for the spectra of produced secondaries based on the fundamental theory and not purely phenomenological. At present the only candidate for this is the hard pomeron model derived from perturbative QCD. Originally constructed for the description of high-energy low- x hadronic scattering (the BFKL model [1]) it has subsequently been generalized to hadronic or deep inelastic scattering on nuclei [2, 3] and nucleus-nucleus scattering [4]. The model suffers from a serious drawback related to the use of fixed and not running strong coupling constant. Curing it does not look too promising, since due to absence of ordering of momenta in the model, it also means solving the confinement problem. However in spite of this defect the model seems to describe high-energy phenomena in a qualitatively reasonable manner. Also attempts to include the running of the coupling in some effective way have shown that the effect of the running is not at all overwhelming, although introduces some quantitative changes into the predictions. So, also for lack of something better, the perturbative QCD pomeron model appears to give a reasonable basis for the discussion of particle production in high-energy heavy-ion collisions. Of course due to the perturbative character of the model it can only give predictions for production of jets, leaving jet-to-hadrons conversion to non-perturbative fragmentation mechanism.

From the start it has to be stressed that heavy-ion collision amplitudes are described in the model by complicated equations, whose solution is quite difficult to obtain even numerically (see [5] for partial results). Happily, as was shown in [6], due to Abramovsky-Gribov-Kancheli

(AGK) cancellations [7], to find the single inclusive distributions one does not have to solve these equations, but only to sum the appropriate sets of fan diagrams, which is accomplished by the non-linear evolution equation of [2, 3]. Still this operation involves a numerical study of considerable complexity. So up to now there has been no consistent calculation of the jet spectra for realistic nuclei, although some preliminary attempts have been done in [8, 9, 10, 11]. In all cases however the authors relied on very drastic simplifications from the start choosing for the nuclear structure and/or for the gluon distributions in the colliding nuclei some primitive explicit forms in accordance with their own taste and prejudice. In fact these forms appear to be rather far from realistic ones, which correspond to actual participants and follow from the calculations. This gave us motivation to calculate numerically the jet spectra in heavy ion collisions as predicted by the hard pomeron model in a consistent manner.

Another goal of the present calculations has been to compare the results obtained on the basis of the expression for the inclusive cross-section which follows from the AGK rules applied to the diagrams with QCD pomerons interacting via the three-pomeron coupling [6] with a somewhat different expression obtained from the colour dipole picture [12]. Our calculations show that these two formally different expressions lead to completely identical results at momenta of the order or higher than the value of the so-called saturation momentum Q_s . At momenta substantially lower than Q_s the colour dipole cross-sections differ from the ones from the AGK rules by a universal constant factor $\sim 0.8 \div 0.9$.

In both cases the spectra at momenta below Q_s are found to be proportional to the number of participants ($\propto A$ for collisions of identical nuclei) and not to the number of collisions ($\propto A^{4/3}$). Since Q_s grows with energy very fast, the region where the spectra are $\propto A$ extends with energy to include all momenta of interest. At momenta greater than Q_s the spectra grow faster than A but still much slower than $A^{4/3}$ (a numerical fit gives something like $\propto A^{1.1}$).

Note that in the last years a few more phenomenologically oriented studies of particle production in nucleus-nucleus production have been presented, in the framework of the color-condensate model [13] solved in the classical approximation on the lattice [10] and in the saturation model [11]. In both approaches quantum evolution of the nuclear gluon density was neglected and the saturation momentum was introduced as a parameter fitted to the experimental data at RHIC. Although some of their predictions (proportionality of the multiplicity to A modulo logarithms) agree with our calculations with full quantum evolutions, the quantitative results are rather different. We postpone a more detailed discussion of this point until our Conclusions.

2 Basic equations

Our basic quantity will be the inclusive cross-section $I_{AB}(y, k)$ to produce a jet with the transverse momentum k at rapidity y in a collision of two nuclei with atomic numbers A and B :

$$I_{AB}(y, k) = \frac{(2\pi)^2 d\sigma}{dy d^2 k}. \quad (1)$$

It can be represented as an integral over the impact parameter b :

$$I_{AB}(y, k) = \int d^2 b I_{AB}(y, k, b). \quad (2)$$

Our study will be restricted to the inclusive cross-sections at fixed impact parameter $b = 0$ (central collisions). We shall also limit ourselves to collisions of identical nuclei $A = B$ and for brevity denote $I_{AA} \equiv I_A$ and so on. The corresponding multiplicity at fixed rapidity y and $b = 0$ will be given by

$$\mu_A(y) = \frac{1}{\sigma_A(b = 0)} \int \frac{d^2 k}{(2\pi)^2} I_A(y, k, b = 0), \quad (3)$$

where $\sigma_A(b)$ is the total inelastic cross-section for the collision of two identical nuclei at fixed impact parameter b . For heavy nuclei one expects that $\sigma_A(b = 0) \simeq 1$, so that the multiplicity is just the integral of the inclusive cross-section over the momenta.

As argued in [4], in the perturbative QCD with a large number of colours the nucleus-nucleus interaction is described by a set of tree diagrams constructed with BFKL pomeron Green functions and triple pomeron vertices for their splitting and fusing. The structure of the interaction at the vertex is illustrated in Fig. 1, in which horizontal lines correspond to real gluons produced in the intermediate states and vertical and inclined lines describe propagating reggeized gluons. From this structure one sees that the produced gluons are contained in the intermediate states of the interacting pomerons, so that to get the inclusive cross-section one has to "open" these pomerons, that is to fix the momentum of one of the intermediate real gluons in them. A similar production mechanism in the old-fashioned local pomeron model was proven to lead to the inclusive cross-section given by a convolution of two sets of fan diagrams connecting the emitted particle to the two nuclei times the vertex for the emission (Fig. 2a). The proof was based on the AGK rules appropriately adjusted for the triple pomeron interaction [14]. It was later shown in [15] that the AGK rules are fulfilled for interacting BFKL pomerons. So the same arguments as in [14] allow to demonstrate that for the collision of two nuclei the inclusive cross-section will be given by the same Fig. 2a, that is, apart from the emission vertex, by the convolution of two sums of fan diagrams, constructed of BFKL pomerons and triple pomeron vertices, propagating from the emitted particle towards the two nuclei [6].

Taking into account the form of the emission vertex (see [6]) we obtain in our case ($A = B$ and fixed $b = 0$)

$$I_A(y, k) = \frac{8N_c\alpha_s}{k^2} \int d^2\beta d^2r e^{ikr} [\Delta\Phi_A(Y - y, r, \beta)][\Delta\Phi_A(y, r, \beta)], \quad (4)$$

Here $\Phi(y, r, \beta)$ is the sum of all fan diagrams connecting the pomeron at rapidity y and of the transverse dimension r with the colliding nuclei at distance β from their centers. One of the nuclei is assumed to be at rest and the other at the overall rapidity Y . Δ 's are the two-dimensional Laplacians applied to Φ 's.

Later from the colour dipole formalism a slightly different form for the inclusive cross-section was derived in [12]. For the dipole-nucleus scattering case it corresponds to changing

$$2\Phi_A(y, \beta, r) \rightarrow 2\Phi_A(y, \beta, r) - \Phi_A^2(y, \beta, r). \quad (5)$$

Note that in [12] it was erroneously stated that the change was from the "quark dipole" Φ to the "gluon dipole" $2\Phi - \Phi^2$. As seen from (5) it is not. In fact the change is equivalent to adding to the AGK contribution (4) a new one which has the meaning of the emission of the gluon from the triple pomeron vertex itself. Such a contribution is not prohibited in principle. From our point of view, taking into account the structure of the vertex shown in Fig. 1, its appearance is difficult to understand. However in this paper we do not pretend to discuss the validity of the two proposed formulas for the inclusive cross-sections on the fundamental level. Rather we shall compare the cross-sections which follow from them after numerical calculations.

For the nucleus-nucleus case the recipe of [12] implies taking into account two new diagrams for the inclusive cross-sections shown in Fig. 2 b and c. As a result one finds, instead of (4), the Kovchegov-Tuchin (KT) cross-section

$$I_A^{KT}(y, k) = \frac{4N_c\alpha_s}{k^2} \int d^2\beta d^2r e^{ikr} [2\Delta\Phi_A(Y - y, r, \beta)\Delta\Phi_A(y, r, \beta) - \Delta\Phi_A(Y - y, r, \beta)\Delta\Phi_A^2(y, r, \beta) - \Delta\Phi_A^2(Y - y, r, \beta)\Delta\Phi_A(y, r, \beta)]. \quad (6)$$

Function $\phi_A(y, r, \beta) = \Phi_A(y, r, \beta)/(2\pi r^2)$, in the momentum space, satisfies the well-known non-linear equation [2, 3]

$$\frac{\partial \phi_A(y, q, \beta)}{\partial \bar{y}} = -H\phi_A(y, q, \beta) - \phi_A^2(y, q, \beta), \quad (7)$$

where $\bar{y} = \bar{\alpha}y$, $\bar{\alpha} = \alpha_s N_c/\pi$, α_s and N_c are the strong coupling constant and the number of colours, respectively, and H is the BFKL Hamiltonian. Eq. (7) has to be solved with an initial condition at $y = 0$ determined by the colour dipole distribution in the nucleon smeared by the profile function of the nucleus. Both cross-sections (4) and (6) can be expressed via function

$$h_A(y, q, \beta) = q^2 \nabla_q^2 \phi_A(y, q, \beta), \quad (8)$$

which has the meaning of internal gluon density in each of the colliding nuclei. One easily obtains for (4)

$$I_A(y, k) = \frac{8N_c \alpha_s}{k^2} \int d^2 \beta d^2 q h_A(Y - y, k - q, \beta) h_A(y, q, \beta). \quad (9)$$

For (6) one also obtains a factorized expression similar to (9)

$$I_A^{KT}(y, k) = \frac{8N_c \alpha_s}{k^2} \int d^2 \beta d^2 q h_A(Y - y, k - q, \beta) [w_A(y, q, \beta) - h_A(y, q, \beta)], \quad (10)$$

where $w_A(y, q, \beta)$ is a new function, which however can be expressed via h_A :

$$w_A(y, k, \beta) = \frac{k^2}{2\pi} \int \frac{d^2 q}{q^2 (k - q)^2} h_A(y, k - q, \beta) h_A(y, q, \beta). \quad (11)$$

Function $h_A(y, k, \beta)$ has a normalization property [6]

$$\int \frac{d^2 k}{k^2} h_A(y, k, \beta) = 1 \quad (12)$$

and at sufficiently high y acquires a scaling property

$$h_A(y, k\beta) = h(k/Q_s(y, \beta)), \quad (13)$$

where $Q_s(y, \beta)$ is the above-mentioned saturation momentum. From (12) and (13) one easily establishes some properties of the new function w_A . Obviously it scales with the same saturation momentum when h_A does

$$w_A(y, k\beta) = w(k/Q_s(y, \beta)). \quad (14)$$

At $k \rightarrow \infty$ it has the asymptotic

$$w_A(y, k, \beta)_{k \rightarrow \infty} \sim 2h_A(y, k, \beta) \quad (15)$$

and finally

$$\int d^2 k w_A(y, k, \beta) = 2 \int d^2 k h_A(y, k, \beta). \quad (16)$$

These properties immediately allow to make some preliminary comparison between the cross-sections given by (4) and (6). Obviously if k/Q_s is large both expressions give the same cross-section due to (16). In the opposite limit of small k/Q_s , the scaling property allows to conclude that the ratio of the two cross-sections is a universal constant which does not depend on y , nor on A nor on β . Our numerical results confirm these predictions.

3 Results

In our study we have taken the initial condition in accordance with the Golec-Biernat distribution [16], duly generalized for the nucleus:

$$\phi_A(0, q, \beta) = -\frac{1}{2}a_A(\beta) \text{Ei}\left(-\frac{q^2}{0.218 \text{GeV}^2}\right), \quad (17)$$

with

$$a_A = 20.8 \text{ mb } AT_A(\beta). \quad (18)$$

where $T_A(\beta)$ is the standard nuclear profile function, which we have taken from the Woods-Saxon nuclear density.

Evolving $\phi_A(y, q, \beta)$ up to values $\bar{y} = 8$ we found the inclusive cross-sections (4) and (6) at center rapidity for energies corresponding to the overall rapidity $Y = \bar{Y}/\bar{\alpha}$, with $\bar{Y} = 16$. Taking $\alpha_s = 0.2$ this gives $Y \sim 80$. This value is far beyond the present possibilities and was chosen only to follow the asymptotical behavior of the cross-sections at super-high energies and compare it with the situation at energies available presently or the near future. The overall cutoffs for integration momenta in Eq.(7) were taken according to $1.10^{-16} \text{GeV}/c < q < 1.10^{+16} \text{GeV}/c$. For the (fixed) value of the strong coupling constant we have taken $\alpha_s = 0.2$

We first discuss the cross-sections (4) obtained from the AGK rules. They are illustrated in Figs. 3-5. To see the absolute values of the inclusive cross-sections at different energies, in Fig. 3 we present them for $A = 9$, $\bar{Y} = 4, 8, 16$ and $y = Y/2$. To illustrate the change of their form with energy, in Fig.4 we present the same distributions at $k > 0.3 \text{ GeV}/c$ normalized to unity and multiplied by k^2 to exclude the trivial $1/k^2$ dependence present in (4),

$$J_9(y, k) = k^2 I_9(y, k) / \int \frac{d^2 k'}{(2\pi)^2} I_9(y, k'), \quad k' > 0.3 \text{ GeV}/c \quad (19)$$

again at $\bar{Y} = 4, 8, 16$. One clearly observes that below a certain point all the momentum dependence is reduced to the trivial factor $1/k^2$, implying that the integral in Eq. (4) is independent of the momentum. This point roughly coincides with the saturation momentum $Q_s(y, \beta)$. However one should have in mind that for a given nucleus the value of the saturation momentum varies depending on the nuclear transverse density at distance β from the center of the nucleus. For $A \geq 9$ and values of β inside the nucleus we find $Q_s \sim 20 \div 200 \text{ GeV}/c$ at $\bar{Y}/2 = 4$ and $Q_s \sim 1.5 \cdot 10^5 \div 1.5 \cdot 10^6$ at $\bar{Y}/2 = 8$. Comparing with Fig. 4 we find that at $k < Q_s$ the integral factor in (4) is practically a constant. For $k > Q_s$ it rapidly falls. At large $k \gg Q_s$ the inclusive cross-sections at the center $y = Y/2$ are found to behave like $1/k^p(y)$ with power $p(y)$ diminishing with energy. From our calculations we approximately find that $p(y) = 3.3, 3.0$ and 2.7 at $\bar{y} = 2, 4$ and 8 respectively. At infinite energies p seems to tend to 2 in correspondence to the fact that $Q_s \rightarrow \infty$

In Fig. 5 we illustrate the A -dependence showing ratios

$$R_A^{part} = \frac{9I_A(y, k)}{AI_9(y, k)} \quad (20)$$

with inclusive cross-sections scaled by A , at $y = Y/2$ and $\bar{Y} = 4, 8$ and 16 (from top to bottom). One clearly sees that whereas at relatively small momenta the inclusive cross-sections are proportional to A , that is to the number of participants, at larger momenta they grow with A faster, however noticeably slower than the number of collisions, roughly as $A^{1.1}$. The interval of momenta for which $I_A \propto A$ can also be related to the value of the saturation momentum $Q_s(y, \beta)$. Inspection of Fig. 5 shows that the distributions are proportional to A at values of k

smaller or in the vicinity of the value of the saturation momentum. Since $Q_s(y, \beta)$ grows with energy, one may conjecture that at infinite energies all the spectrum will be proportional to A .

Passing to the determination of multiplicities one has to observe certain care because of the properties of the perturbative QCD solution in the leading approximation embodied in Eqs. (4) and (7). As follows from (4) the inclusive cross-section blows up at $k^2 \rightarrow 0$ independently of rapidity y . So the corresponding total multiplicity diverges logarithmically. However, the physical sense has only emission of jets with high enough transverse momenta. Thus one has to cut the spectrum from below by some k_{min} which separates the spectrum of jets proper from soft gluons which are not related to jets. Inevitably the multiplicity of thus defined jets depends on the chosen value of k_{min} . We have chosen $k_{min} = 2$ GeV/c. At all energies the multiplicities at the center $\mu_A(y = Y/2)$ were found to be approximately proportional to A . The ratios $\mu_A(y = Y/2)/A$ are presented in Fig. 6. One observes that their values are quite high and grow very fast with energies. This is not surprising, considering a very high value of the pomeron intercept in the lowest order BFKL model. The bulk of the multiplicity comes from jets with relatively high momenta. To illustrate this point in Fig. 7 we show the dependence of the central multiplicity on k_{min} for $A = 9$ and at $\bar{Y} = 8$ in the interval $k_{min} = 0.3 \div 16$ GeV/c. One observes that it goes down very slowly, indicating that it is the high momentum tail of the distribution which matters.

Finally we pass to the cross-sections obtained with the KT formula (6). In Fig. 8 we show the ratios of these cross-sections to the ones defined by the AGK rules, Eq. (4), for $y = Y/2$ and $\bar{Y} = 4, 8$ and 16 . These ratios turn to unity at k in the vicinity and above Q_s , as discussed in the end of the preceding section. Below Q_s the ratios are approximately equal to $0.8 \div 0.9$ with little dependence on A and Y . Some dependence which is left can be explained by the fact that for very peripheral parts of the nucleus the scaling regime can only be reached at rapidities well above the considered ones. Due to this very simple relation between the two cross-sections, all conclusions about the A -dependence drawn for the AGK cross-section (4) remain valid also for the KT cross-section (6).

4 Conclusions

We have calculated the inclusive cross-sections for gluon production at mid-rapidity in nucleus-nucleus central collisions in the perturbative QCD approach with a large number of colors. Realistic nuclear densities were employed to account for the peripheral parts of the nuclei, whose contribution rapidly grows with energy due to smallness of unitarizing non-linear effects. The form of the cross-sections is found to be determined by the value of the saturation momentum Q_s , which depends on the rapidity and nuclear density. At momenta much lower than Q_s the spectrum is proportional to $1/k^2$. Its A dependence is close to linear. At momenta much higher than Q_s the spectrum is found to fall approximately as $1/k^{2.7 \div 3.3}$ with the A -dependence as $\sim A^{1.1}$. The multiplicities at mid-rapidity are found to be proportional to A with a good precision. They grow with energy very fast which is related to a fast growth of the saturation momentum.

We also compared two different forms for the inclusive cross-section, which follow from the AGK rules or the dipole picture. The difference between their predictions was found to be absent for values of momenta larger than Q_s . At momenta smaller than Q_s the difference reduces to a universal constant factor: the dipole cross-sections are just $0.8 \div 0.9$ of the AGK cross-sections. With the growth of Y and/or A this factor slowly grows towards unity, so that it is not excluded that at infinite A and Y the two cross-sections (4) and (6) totally coincide at all values of momenta. All our conclusions about the energy, momentum and A dependence are equally valid for both forms of the inclusive cross-sections.

As mentioned in the Introduction a few more phenomenological studies of the gluon pro-

duction in nucleus-nucleus collisions were recently made in the classical approximation to the colour-glass condensate model [10] and in the saturation model of [11]. In both studies quantum evolution was neglected, so that scaling with the saturation momentum Q_s was postulated rather than derived. The saturation momentum thus appeared as an external parameter, whose A and Y dependence were chosen on general grounds and whose values were fitted to the experimental data at RHIC. In both models the multiplicities turned out to be proportional to the number of participants (modulo logarithmic dependence on A different in the two approaches). This agrees with our results. However the form of the inclusive distributions in momenta found in [10] is different from ours. Its behaviour both at small k ($\sim 1/\sqrt{k^2 + m^2}$ with $m = 0.0358Q_s$) and at large k ($\sim 1/k^4$) disagrees with the form of the spectrum we have found. For realistic nuclei the spectrum was calculated in [10] only up to $6 \div 7$ GeV/c, so it is not possible to see if any change in its A -behaviour will occur at higher momenta. But most of all, the value of the saturation momentum and the speed of its growth with rapidity which we have found from the QCD pomeron model with full quantum evolution are much larger than the fitted values in both [10] and [11]. This is no wonder in view of a very high value of the BFKL intercept in the leading approximation. From the phenomenological point of view this is the main drawback of the BFKL theory. To cure it one possibly has to include higher orders of the perturbation expansion and the running coupling constant. Although some work in this direction has been done for linear evolution [17], no attempts to generalize this to non-linear evolution in some rigour has been made yet.

5 Acknowledgements

The author is deeply indebted to Yu.Kovchegov for a constructive discussion and valuable comments and to N.Armesto and B.Vlahovic for their interest in this work. This work has been supported by a NATO Grant PST.CLG.980287.

References

- [1] E.A.Kuraev, L.N.Lipatov and V.S.Fadin, Sov. Phys. JETP **45** (1977) 199; Ya.Ya.Balitsky and L.N.Lipatov, Sov. J.Nucl.Phys. **28** (1978) 22.
- [2] Yu.V.Kovchegov, Phys. Rev. **D 60** (1999) 034008; **D 61** (2000) 074018.
- [3] M.A.Braun, Eur. Phys. J. **C 16** (2000) 337.
- [4] M.A.Braun, Phys. Lett. **B 483** (2000) 115.
- [5] M.A.Braun, hep-ph/0309293, to be published in Eur. Phys. J. C.
- [6] M.A.Braun, Phys. Lett. **B 483** (2000) 105.
- [7] V.A.Abramovsky, V.N.Gribov and O.V.Kancheli, Sov. J. Nucl. Phys. **18** (1974) 308
- [8] J.L.albacete, N.Armesto, A.Kovner, C.A.salgado and U.A.Wiedemann, Phys. Rev. Lett **92** (2004) 082001
- [9] D.Kharzeev, Yu.Kovchegov and K.Tuchin, hep-ph/0405045
- [10] A.Krasnitz, Y.Nara and R.Venugopalan, Phys. Rev. Lett **87** (2001) 192302; Nucl. Phys. **A 717** (2003) 268.
- [11] D.Kharzeev and M.Nardi, Phys.Lett. **B 507** (2001) 121; D.Kharzeev and E.Levin, Phys. Lett. **B 523** (2001) 79.
- [12] Yu. Kovchegov and K.Tuchin, Phys. Rev. D 65 (2002) 074026.
- [13] L.D.McLerran and R.Venugopalan, Phys. Rev. **D 49** (1994) 2233, 3352; **D 50** (1994) 2225; E.G.Ferreiro, E.Iancu, A.Leonidov and L.D.McLerran, Nucl. Phys. **A 710** (????) 5414.
- [14] M.Ciafaloni *et al.*, Nucl. Phys. **B 98** (1975) 493.
- [15] J.Bartels and M.Wuesthoff, Z.Physik, **C 66** (1995) 157.
- [16] K.Golec-Biernat and M.Wuesthoff, Phys. Rev. **D 59** (1999) 014017; **D 60** (2000) 114023.
- [17] V.S.Fadin and L.N.Lipatov, Phys. Lett. **B 429** (1998) 127; G.Camici and M.Ciafaloni, Phys. Lett. **B 412** (1998) 396; **B 430** (1998) 349.

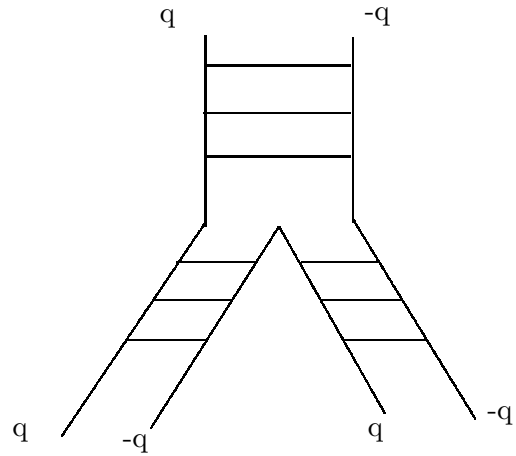


Figure 1: Interaction of three BFKL pomerons at the splitting vertex

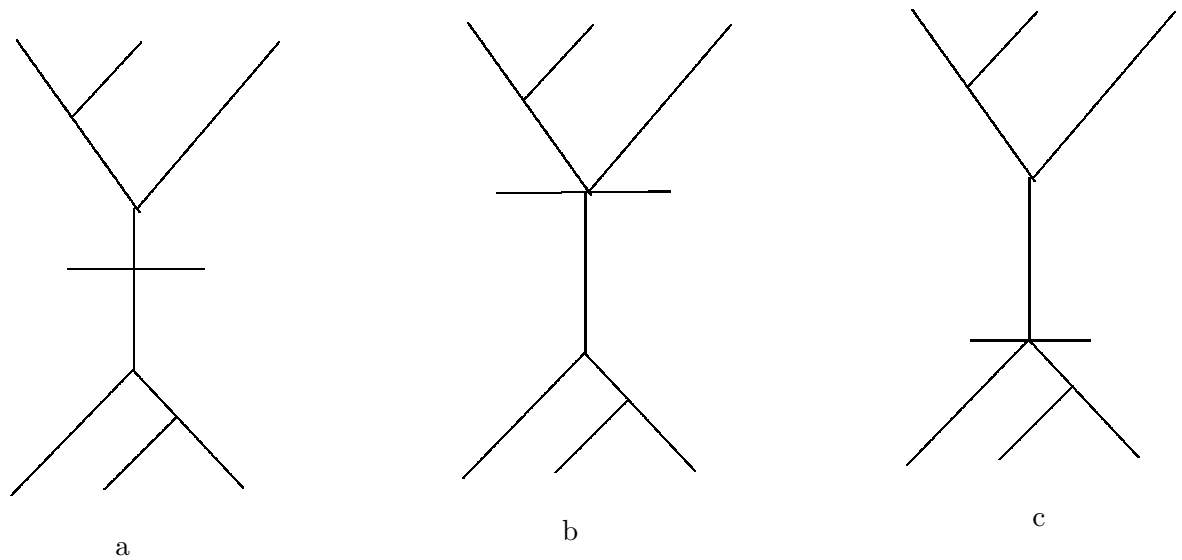


Figure 2: Typical diagrams for the inclusive cross-section in nucleus-nucleus collisions.

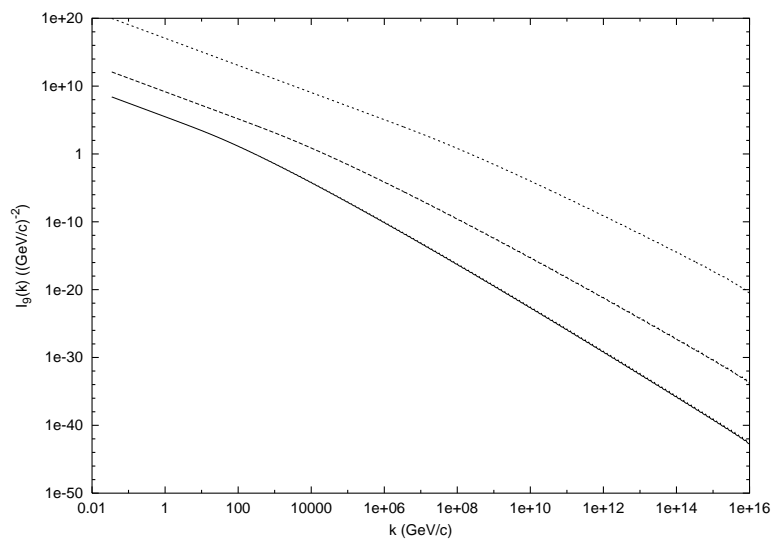


Figure 3: Inclusive cross-sections $I_9(y, k)$ at $y = \frac{Y}{2}$. Curves from top to bottom at small k correspond to scaled overall rapidities $Y = 4, 8, 16$.

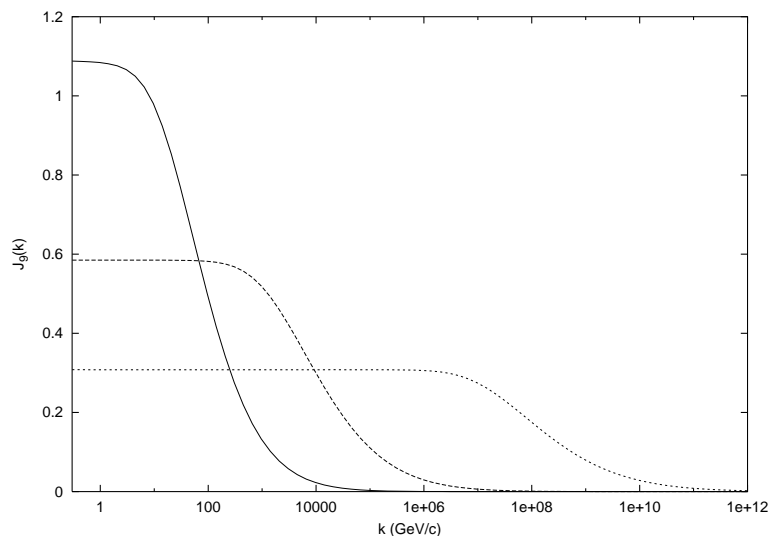


Figure 4: Normalized distributions $J_9(y, k)$ (Eq. (25)) at $y = \frac{Y}{2}$. Curves from top to bottom at small k correspond to scaled overall rapidities $\bar{Y} = 4, 8, 16$.

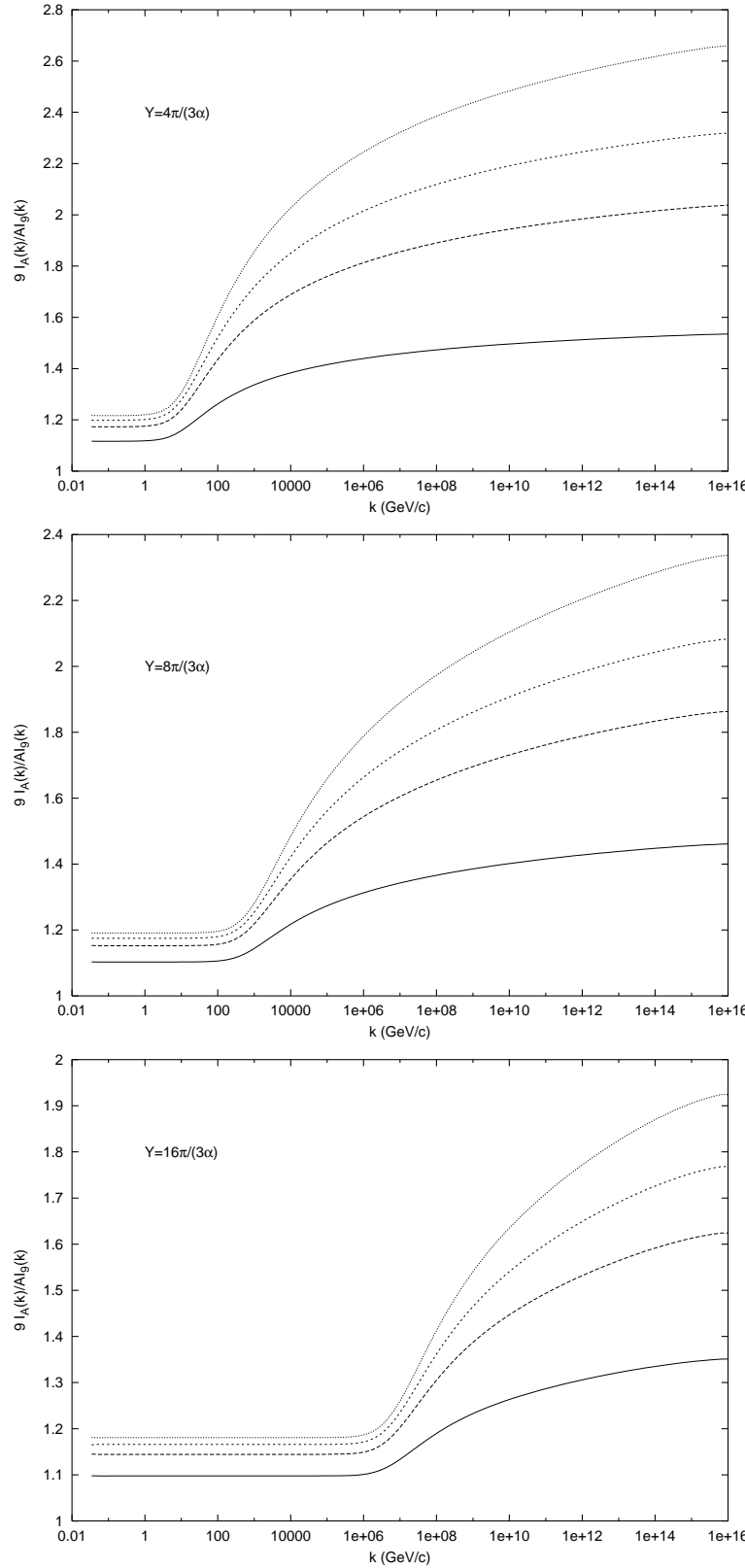


Figure 5: From top to bottom: A-dependence of momentum distributions, scaled with the number of participants, at $\bar{Y} = 4, 8, 16$. Curves from bottom to top show ratios $9I_A(y, k)/AI_9(y, k)$ at center rapidity ($y = \frac{Y}{2}$) for $A = 9, 27, 64, 108$ and 180 .

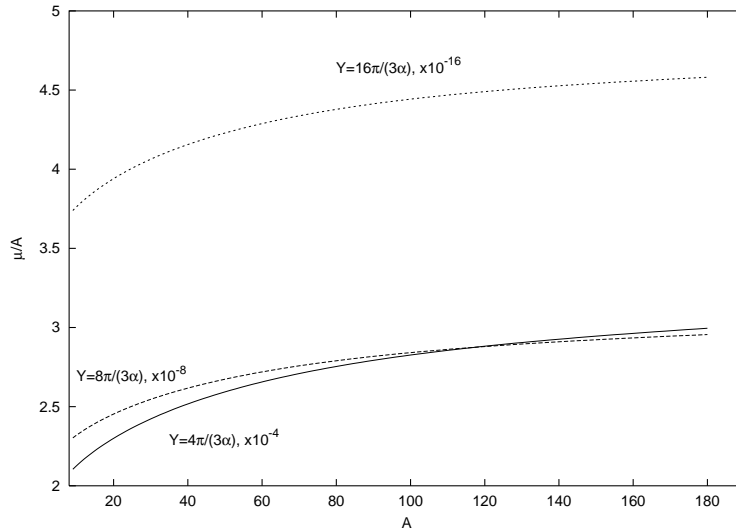


Figure 6: From top to bottom: A-dependence of multiplicities, scaled with the number of participants, at $\bar{Y} = 4, 8, 16$. Curves from bottom to top show $\mu_A(y)/A$ at center rapidity ($y = \frac{Y}{2}$) for $A = 9, 27, 64, 108$ and 180 .

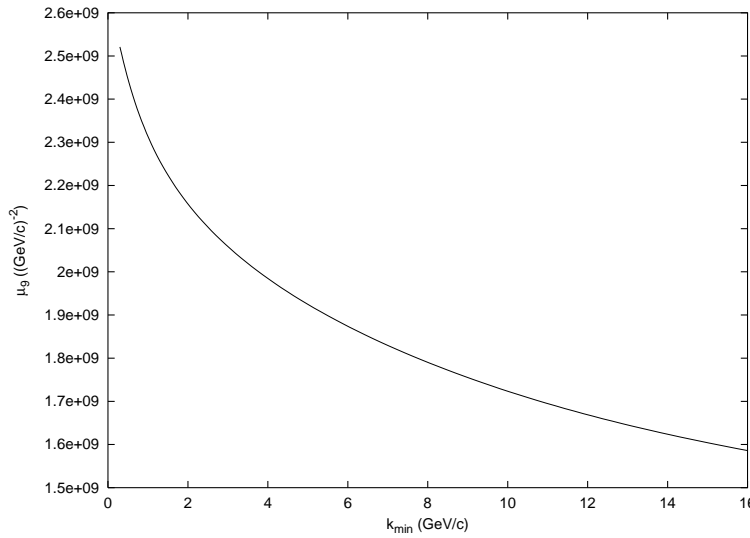


Figure 7: The dependence of multiplicity for $A = 9$ at center rapidity and $\bar{Y} = 8$ on the infrared cut k_{min}

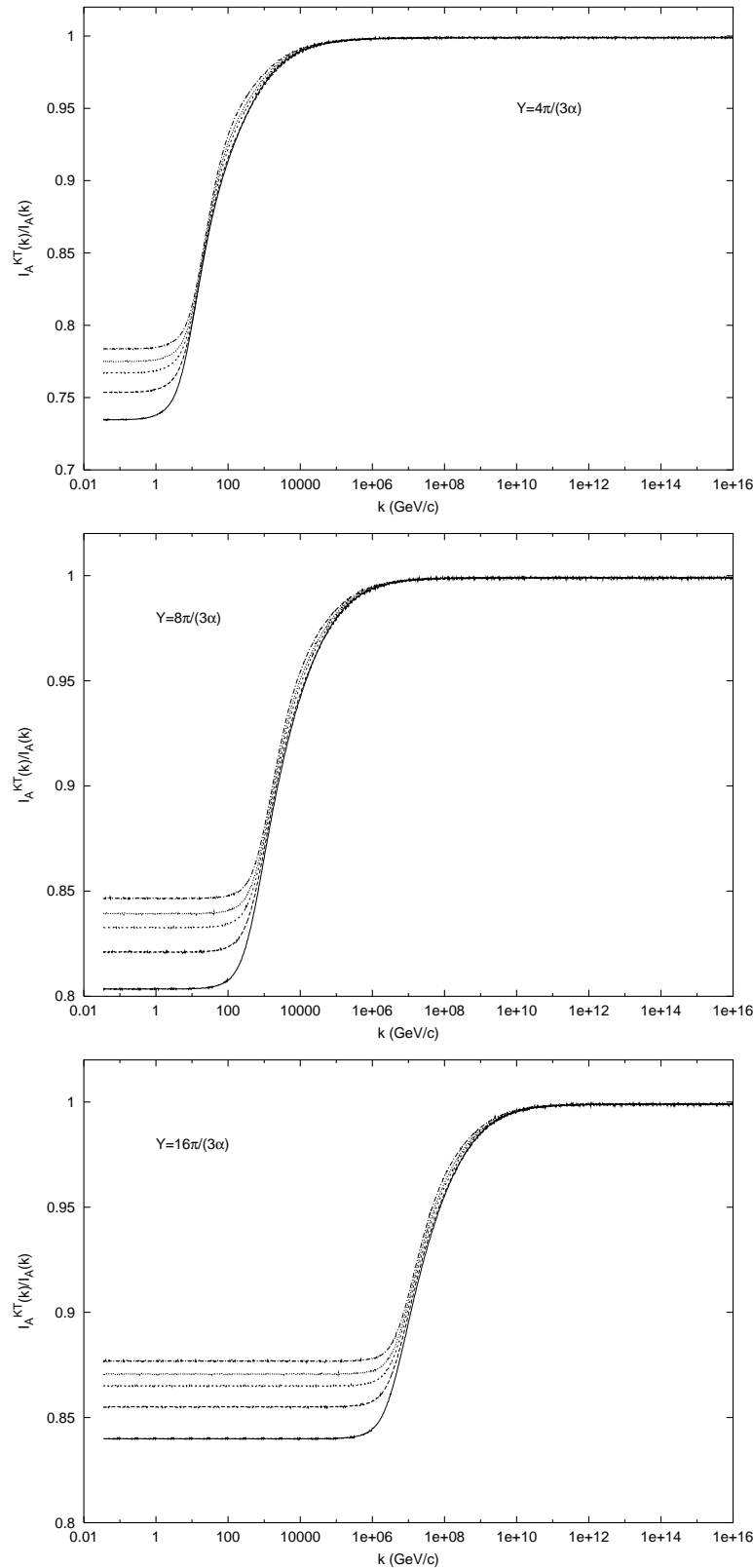


Figure 8: Ratios of the KT inclusive cross-sections, Eq. (6), to the ones found from the AGK rules, Eq. (4) at center rapidity ($y = Y/2$) and $\bar{Y} = 4, 8, 16$. Curves from bottom to top refer to $A = 9, 27, 64, 108$ and 180